

Characterization of the Effects of Hyperbaric Oxygen on the Biochemical and Optical Properties of the Bovine Lens

Julie C. Lim,^{1,2} Ehsan Vaghefi,² Bo Li,¹ Mitchell G. Nye-Wood,^{1,2} and Paul J. Donaldson^{1,2}

¹Department of Physiology, School of Medical Sciences, NZ National Eye Centre, University of Auckland, New Zealand

²School of Optometry and Vision Science, NZ National Eye Centre, University of Auckland, New Zealand

Correspondence: Julie C. Lim, Department of Physiology, School of Medical Sciences, University of Auckland, New Zealand; j.lim@auckland.ac.nz.

Submitted: January 14, 2016

Accepted: March 10, 2016

Citation: Lim JC, Vaghefi E, Li B, Nye-Wood MG, Donaldson PJ. Characterization of the effects of hyperbaric oxygen on the biochemical and optical properties of the bovine lens. *Invest Ophthalmol Vis Sci*. 2016;57:1961–1973. DOI:10.1167/iov.16-19142

PURPOSE. To assess the morphologic, biochemical, and optical properties of bovine lenses treated with hyperbaric oxygen.

METHODS. Lenses were exposed to hyperbaric nitrogen (HBN) or hyperbaric oxygen (HBO) for 5 or 15 hours, lens transparency was assessed using bright field microscopy and lens morphology was visualized using confocal microscopy. Lenses were dissected into the outer cortex, inner cortex, and core, and glutathione (GSH) and malondialdehyde (MDA) measured. Gel electrophoresis and Western blotting were used to detect high molecular weight aggregates (HMW) and glutathione mixed protein disulfides (PSSG). T2-weighted MRI was used to measure lens geometry and map the water/protein ratio to allow gradient refractive index (GRIN) profiles to be calculated. Optical modeling software calculated the change in lens optical power, and an anatomically correct model of the light pathway of the bovine eye was used to determine the effects of HBN and HBO on focal length and overall image quality.

RESULTS. Lenses were transparent and lens morphology similar between HBN- and HBO-treated lenses. At 5- and 15-hour HBO exposure, GSH and GSSG were depleted and MDA increased in the core. Glutathione mixed protein disulfides were detected in the outer and inner cortex only with no appearance of HMW. Optical changes were detectable only with 15-hour HBO treatment with a decrease in the refractive index of the core, slightly reduced lens thickness, and an increase in optimal focal length, consistent with a hyperopic shift.

CONCLUSIONS. This system may serve as a model to study changes that occur with advanced aging rather than nuclear cataract formation per se.

Keywords: hyperbaric oxygen, oxidative damage, optical changes

Age-related nuclear (ARN) cataract is the leading cause of blindness worldwide¹ and is associated with protein modifications caused by oxidative damage to the lens.² With advancing age, there is significant depletion of the antioxidant glutathione (GSH) specifically in the lens core, which renders proteins within this region susceptible to oxidative damage.² Animal models have been developed to mimic the cataractogenic process as a means of testing the efficacy of various antioxidants to slow down, or prevent the progression of cataract.³ However, the results of these studies have been somewhat limited, mostly due to lack of scientific rationale behind the selection of the compound being tested, and second, by the selection of the animal chosen that is presumed to best replicate the changes that occur in human ARN cataract.

High-pressure or hyperbaric oxygen (HBO) has long been used as therapy in humans for decompression sickness,⁴ air embolisms,⁵ and accelerating healing of diabetic wounds.^{6,7} A side effect of this treatment was the development of nuclear cataract or increased nuclear light scattering.⁸ As a result of this finding, HBO has been used to induce cataract in animals (in vitro and in vivo) to enable the mechanisms of ARN cataract to be studied. In vivo studies of HBO-induced cataracts in older guinea pigs (17–18 months) revealed biochemical changes in the lens nucleus consistent with an increased state of oxidative stress in these animals.⁹ These changes included markedly

higher levels of oxidized protein thiols and mixed disulfides,⁹ a depletion of GSH in the lens nucleus (~30%) that was not apparent in the cortex,⁹ a decrease in water-soluble proteins,⁹ and increased products of lipid oxidation.¹⁰ Large disulfide cross-linked protein aggregates containing alphaA-, beta-, gamma-, and zeta-crystallins also were detected in the lens nucleus,¹¹ and these protein aggregates were of similar size to those found in human nuclear cataracts.¹² Lenses from these HBO-treated animals were hazy in appearance and showed increased nuclear light scattering, but did not exhibit the dense nuclear opacity associated with ARN cataract in humans.⁹ Similar biochemical changes, such as GSH depletion in the lens nucleus¹³ and increased mixed disulfide formation,^{14,15} also were induced in vitro by the acute exposure of organ-cultured rabbit lenses to HBO. Thus, it appears that both in vivo and in vitro exposure of lenses to HBO can mimic biochemical changes that precede ARN cataract formation in humans.

In this study, we wanted to develop an in vitro HBO model of nuclear cataract that used bovine lenses, and then test whether this specific animal model replicates the biochemical and optical changes that precede cataract formation in the human lens. We selected bovine lenses rather than the commonly used rabbit lenses for our study, as not only are these lenses readily obtained from local abattoirs, but the larger size of the bovine lens provides sufficient quantities of tissue



for biochemical and Western blot analysis. Furthermore, the larger size of the bovine was compatible with magnetic resonance imaging (MRI) analysis in which protocols for imaging bovine lenses had already been established in our laboratory.¹⁶ In previous work, Vaghefi et al.¹⁷ developed MRI methodologies to visualize the lens circulation system in normal bovine lenses and demonstrated that the circulation system is responsible for actively removing water from the lens center. Subsequently, they showed that active removal of water maintains a low-water/high-protein ratio in the lens core¹⁶ that in turn establishes a gradient of refractive index (GRIN), which is essential for maintaining good vision.¹⁸ Using these established MRI parameters, we are able to extend our biochemical analysis of HBO-treated bovine lenses to investigate correlations of the effects of HBO on optical properties of the lens and determine the validity of the HBO system as a model of nuclear cataract.

MATERIALS AND METHODS

Animals

Young fresh whole cow eyes (18–24 months) were collected from the local abattoir (Auckland Meat Processors, Otahuhu, New Zealand). Lenses were dissected from the eye and any remnants of the iris and vitreous humor removed by rolling on filter paper.

Hyperbaric Gas Treatment

Lenses undergoing hyperbaric nitrogen (HBN) or HBO treatment were placed anterior side up in 250-mL containers containing 25 mL Medium 199 (M199 with HEPES buffer, L-glutamine, and phenol red) supplemented with 1% antibiotics (penicillin, streptomycin, and neomycin) prewarmed to 37°C. Before culture, the containers were covered in a layer of parafilm and punctured to create 8 to 10 small holes. Lenses were then exposed to either 100% nitrogen (HBN; pressure control group) or 100% oxygen (HBO) at a pressure of 100 atm for 5 hours or 15 hours (1850-mL Cell Disruption Vessel, model 4636; Parr Instrument Company, Moline, IL, USA), based on experimental conditions described by Cappiello and colleagues.¹⁴ The interior chamber of the vessel was maintained at 37°C by partial immersion of the instrument into a temperature-controlled water bath. Following treatment, complete depressurization was conducted over a 30-minute period to avoid the possible dangers of freezing that can occur during rapid decompression. Lenses were then removed from their containers and imaged using a stereomicroscope (Stemi SV11; Carl Zeiss, Thornwood, NY, USA) to assess lens transparency. For biochemical analyses, 5-hour HBN/HBO, 15-hour HBN/HBO-treated lenses or lenses freshly dissected from the cow (untreated) were flash-frozen in liquid nitrogen and then stored at –80°C until ready for further use. For MRI analyses, 5-hour HBN/HBO, 15-hour HBN/HBO-treated lenses or lenses cultured in artificial aqueous humor solution (AAH-NaCl, 125 mM; KCl 4.5 mM; MgCl₂ 0.5 mM; CaCl₂ 2 mM; NaHCO₃ 10 mM; glucose 5 mM; sucrose 20 mM; buffered with 10 mM HEPES to pH 7.1) for 5 hours or 15 hours were placed in sample holders with their anterior surfaces facing up. Lenses were then subjected to T2 mapping MRI according to previously established protocols.¹⁶ Each MRI data set took approximately 45 minutes to collect. Maps of refractive index were generated (see the section “T2-Weighted Imaging of Bovine Lenses”) and analyzed by optical modeling (see the section “Optical Modeling”) using established parameters optimized in our laboratory.¹⁶

Lens Tissue Preparation for Biochemical Analyses

Decapsulated bovine lenses were dissected into the outer cortex, the inner cortex, and the core regions following immediate removal from the eye (untreated) or following 5-hour HBN/HBO or 15-hour HBN/HBO treatment. Currently there is no empirical data distinction among these three regions and the five different zones of the bovine lens described by al-Ghoul and Costello.¹⁹ Therefore, lenses were dissected with sharpened tweezers into the three distinct zones based on their physical properties. The superficial layers of fiber cells composed of cortical-differentiating fiber cells were peeled away and pooled as the outer cortex fraction (~40% total lens mass). The remaining inner cortical fiber cells encompassing cells in the adult nucleus were removed and pooled as the inner cortex fraction (~30% total lens mass). The remaining hard mass of tissue, which included the juvenile, fetal, and embryonic nucleus, was retained as the core fraction (~25%–30% of total lens mass). For biochemical assays (GSH/oxidized glutathione [GSSG] and malondialdehyde [MDA] analysis), each fraction was then homogenized in 1.75 mL EDTA (50 mM) using an electrical drill with fitted head pieces and then centrifuged at 13,200g for 20 minutes at 4°C. The supernatant was then collected and used for GSH/GSSG or MDA determination. For Western blot analysis, each fraction was homogenized in 5 mM Tris-HCl, 5 mM EDTA, and 5 mM EGTA (pH 8.0) using an electric drill, and then centrifuged at 13,200g for 20 minutes at 4°C. The supernatant was collected and retained as the water-soluble (WS) fraction at –80°C. The pellet was then washed three times in storage solution (5 mM Tris-HCl, 2 mM EDTA, 2 mM EGTA, 100 mM NaCl) with centrifugation. The washed pellet was then mixed with 7 M urea and centrifuged at 13,200g for 20 minutes at 4°C. The supernatant was collected and retained as the urea-soluble (US) fraction at –80°C. The concentration of proteins was determined with a Pierce 660-nm protein assay kit (ThermoScientific, Rockford, IL, USA).

Glutathione/GSSG Determination

Glutathione is the principal antioxidant in the lens and is considered to be one of the most important scavengers of reactive oxygen species.²⁰ The measurement of GSH and GSSG within cells is often used as a marker of oxidative stress with depletion of reduced GSH and a concomitant increase in GSSG considered initiating factors in the pathogenesis of cataract development. Reduced (GSH), oxidized (GSSG), and total GSH (GSH+GSSG) were measured by a GSH assay adapted from the Glutathione (GSH/GSSG/Total) Fluorometric Assay kit (Biovision, Milpitas, CA, USA). This assay uses the nonfluorescent probe ophthalaldehyde (OPA) to react with thiol groups, such as contained in GSH, to form a highly fluorescent isoindole derivative. All samples and standards were carefully handled on ice throughout all the steps so as to avoid autoxidation of the reduced thiols. Sixty microliters of collected supernatant was mixed in 20 μ L 19.5% wt/vol trichloroacetic acid (TCA), vortexed, and centrifuged at 13,200g for 4 minutes at 4°C. The resultant supernatant (40 μ L) was then mixed with 20 μ L ice-cold 3 N potassium hydroxide to precipitate the TCA and neutralize the samples; 10 μ L of samples were added to individual wells on a black 96-well clear-bottom fluorescence plate, containing 80 μ L buffer solution (0.1 M NaHCO₃, 46.5 mM PBS, 0.17 M NaOH [pH 13.5]). In parallel, the total GSH in each sample and standard was measured by additional incubation with 10 μ L 0.02 M Tris (2-carboxyethyl) phosphine (TCEP), a reducing agent that reduces GSSG to GSH, for 10 minutes at room temperature. All samples were then fluorescently derivatized with 10 μ L 1% wt/vol OPA in methanol.

The plate was incubated in the dark for 40 minutes at room temperature and fluorescence measured at optimal wavelengths (excitation 340 nm and emission 420 nm) for OPA-thiol adducts using a microplate reader (SpectraMax M2; Molecular Devices, Sunnyvale, CA, USA). Total GSH and GSSG concentrations were determined using GSH and GSSG standard curves as per the manufacturer's instructions. Glutathione disulfide concentrations were calculated based on the difference between total GSH and reduced GSH values.

Malondialdehyde Assay

Malondialdehyde is one of the most prevalent by-products of lipid peroxidation and a common marker of oxidative stress.²¹ Malondialdehyde levels in the lens were measured by determining the thiobarbituric acid reactive substance concentrations from the collected supernatants. Briefly, to 0.1 mL of the supernatant or standard, 0.1 mL 8.1% SDS lysis solution was added, the sample vortexed, and incubated for 5 minutes at room temperature. Next, 0.25 mL thiobarbituric acid (TBA) reagent (0.52% TBA in 20% acetic acid, pH 3.5) was added, vortexed, and then incubated in a 95°C water bath for 45 minutes. After cooling, the samples were centrifuged at 10,000g for 15 minutes; 0.3 mL of the supernatant was then removed and placed in an equal volume of N-butanol, vortexed for 60 seconds and then centrifuged for 5 minutes at 10,000g. Then, 150 µL of the organic fraction (top layer) was transferred to a transparent 96-well plate and fluorescence was measured with excitation at 540 nm and emission at 590 nm. Malondialdehyde concentrations were calculated by using MDA as a standard.

Immunohistochemistry

To examine lens morphology, bovine lenses were fixed either immediately after dissection from the eye (untreated) or following HBN or HBO treatment in 10% paraformaldehyde for 7 days at room temperature. Following fixation, lenses were washed in PBS and cryoprotected by incubation in 10% sucrose-PBS for 1 hour, 20% sucrose-PBS for 1 hour, and then 30% sucrose-PBS overnight at 4°C. For sectioning, lenses were mounted in an equatorial orientation on prechilled chucks and encased in Tissue-Tek optimum cutting temperature compound. Lenses were cryosectioned into 14-µm-thick sections and transferred onto superfrost-coated microscope slides (Superfrost Plus; ESCO, Electron Microscopy Sciences, Fort Washington, PA, USA). Sections were washed three times in PBS and then cell membranes labeled with a fluorescein-conjugated wheat germ agglutinin (WGA-TRITC). After extensive washing in PBS, sections were mounted in antifading reagent (Citifluor; AFI, Canterbury, UK) and viewed with a confocal laser scanning microscope (FV-1000; Leica, Heidelberg, Germany). Images were pseudo-colored using Adobe Photoshop software (Adobe Systems, Inc., San Jose, CA, USA).

Sodium Dodecyl Sulfate–Gel Electrophoresis and Western Blot Analysis

Fifteen micrograms of protein was incubated in loading dye without β-mercaptoethanol and separated on a 10% SDS-PAGE gel. To visualize the appearance of high-molecular-weight (HMW) proteins, gels were stained in Coomassie Brilliant Blue R250 dye for 30 minutes at room temperature with rocking, and then destained overnight in a 50/50/10 vol/vol/vol mix of water, methanol, and acetic acid. To detect glutathione mixed protein disulfides (PSSG), following gel electrophoresis, protein bands were transferred to a polyvinylidene difluoride membrane by electrophoresis for 40 minutes at 170 mA. The

membrane was incubated with blocking solution (5% milk in 1 × Tris-buffered saline [TBS; 2 mM Tris-HCl, 140 mM NaCl, pH 7.6]) at room temperature for 1 hour. The protein blots were incubated overnight with PSSG antibodies (1:1000) or β-actin antibodies (1:10,000) to confirm equal loading, followed by incubation with anti-mouse or anti-rabbit horseradish peroxidase secondary antibody (1:10,000; Amersham, GE Healthcare, Waukesha, WI, USA) for 1 hour each. After incubation, the membrane was washed three times for 10 minutes in 1 × TBS. Labeled protein was visualized by chemiluminescence detection (ECL Prime; Amersham) and bands visualized using a FujiFilm LAS-4000 Scanner (Fujifilm Life Science, Stamford, CT). Image J analysis was used to quantify pixel intensity of the PSSG bands.

T2-Weighted Imaging of Bovine Lenses

Because the refractive index of the lens (GRIN) is directly related to its water content and protein concentration,¹⁶ we measured the water-to-protein ratio from a T2 constant calculation by MRI. Briefly, a Varian Unity Inova 4.7-T horizontal bore MRI system (Varian, Inc., Palo Alto, CA, USA), equipped with a 65-mm internal diameter (ID) and a 100 G/cm gradient system was used. Untreated lenses (bovine lenses cultured for 5 or 15 hours in M199) or HBN- or HBO-treated lenses were imaged using a 40-mm ID RF probe and a spin-echo pulse sequence as follows: repetition time = 2 seconds, echo time (TE) = 6.7 ms, inversion time = 200 ms, slice thickness = 1 mm, field of view = 24 × 24 mm, matrix size = 256 × 256, in-plane resolution = 93 µm. The geometric parameters of the lens (front and back radii of curvature), and conic constants, axial length, and equatorial radius, were extracted from the MRI T2-weighted images using the common filtering and masking methods (MATLAB Image Processing Toolbox; The MathWorks, Inc., Natick, MA, USA). By performing the spin-echo sequence using a train of TE values (7.5, 8, 10, 12, 15, 18, 22, 30, 40, and 45 ms), we were able to create a dataset of 10 T2-weighted signal points for each pixel within the image. Next, the T2 constants were extracted from the T2-weighted image series, and by repeating the process for all pixels within an image, a two-dimensional map of T2 values for each lens and experimental condition could be constructed. Because T2 constants are inversely proportional to refractive index ($n \sim 1/T2$),^{22,23} a GRIN profile of each lens was created by using the equation:

$$n = -5.5778 \times (1/T2)^2 + 1.1284 \times (1/T2) + 1.3784$$

where n is the unitless refractive index and the T2 values are in milliseconds. Geometrical and T2 constant measurements were performed on six lenses ($n = 6$) from each experimental group so as to ensure the statistical significance of the results.¹⁶

Optical Modeling

The commercial optical modeling software package ZEMAX (Development Corp., San Diego, CA, USA), which uses Snell's law²⁴ to simulate light ray propagation through optical devices, was first used to assess the optical properties of lenses cultured under different conditions and then to simulate what effect the changes in lens properties had on the overall vision quality using protocols established in an earlier study.¹⁶ Briefly, the average geometric parameters (front and back radii of curvature, conic constants, axial length, and equatorial radius) and the GRIN obtained by T2 imaging of untreated bovine lenses, or lenses cultured in either HBN or HBO for 5 hours and 15 hours were used by ZEMAX to calculate the optical power

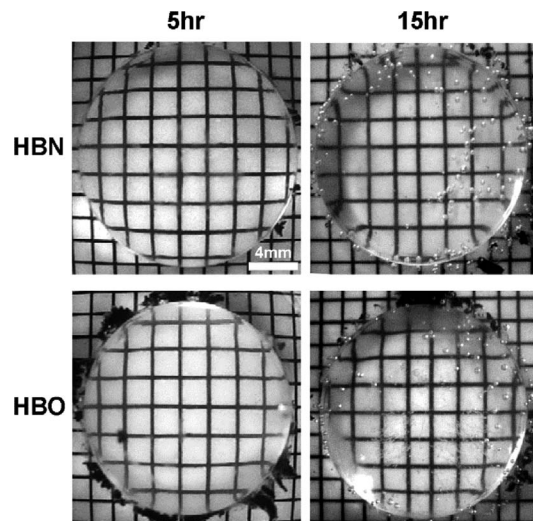


FIGURE 1. Effect of HBN and HBO on the transparency of organ-cultured bovine lenses. Bright field images revealed no signs of cataracts or grid irregularities between the two groups. Scale bar: 4 mm.

(diopters) of lenses in the different experimental conditions. To simulate how HBO-induced changes to the optical properties of the lens affects overall vision quality, a ZEMAX model of the bovine eye developed by Vaghefi et al.¹⁶ was solved using the average optical properties calculated for lenses incubated for 15 hours in either HBN or HBO. The model used a fixed pupil diameter of 2 mm and a polychromatic (wavelengths = 486, 587, and 656 nm) light source.²⁵ For each experimental condition, the model was solved for two different focal lengths: an optimum focal length of the optical pathway formed by the eye that results in the formation of the sharpest final image, or with the focal length set to the vitreous chamber thickness (V_T), to assess the quality of image formation on the retina.

Statistical Analysis

Statistical analysis was performed using either MATLAB (The MathWorks, Inc.) or GraphPad Prism, version 6.05 (GraphPad Software, Inc., San Diego, CA, USA). For analysis of the data obtained from the GSH and MDA assay, 2-way ANOVA was used. For analysis of PSSG pixel density, the Mann-Whitney test was used. In all analyses, a P value less than 0.05 was deemed to be statistically significant. All error bars are presented as the mean \pm SEM, with statistical significance displayed as * P < 0.05, ** P < 0.01, *** P < 0.001.

RESULTS

Effects of HBO on Lens Transparency and Fiber Cell Morphology

Transparency. Lenses treated with HBN or HBO for 5 hours or 15 hours were clear and transparent with no distortion of the underlying grid (Fig. 1), similar to that seen for untreated lenses (data not shown). The absence of a dense nuclear cataract following HBO exposure is similar to the findings by Giblin and colleagues,^{9,13} who have shown that nuclear cataracts do not develop in either the in vivo guinea pig lens or in vitro rabbit lens HBO models.

Morphology. Lens morphology was examined on untreated lenses and compared with lenses following hyperbaric

treatment (Fig. 2). The morphology of the cells in the outer cortex (OC), adult nucleus (AN), juvenile nucleus (JN), fetal nucleus (FN), and embryonic nucleus (EN) revealed no obvious changes in lens morphology as a result of exposure to HBN or HBO (Fig. 2). This is consistent with findings between normal and human nuclear cataractous lenses in which the morphology of the nuclear regions was indistinguishable.^{26,27}

Effects of HBO on Lens Antioxidant Levels and Protein Biochemistry

Glutathione Levels. Because GSH is known to be the first defense system against oxidative stress, we measured the levels of reduced GSH in the OC, inner cortex (IC), and core regions of untreated lenses and lenses treated for 5 hours or 15 hours in HBN or HBO (Fig. 3A). In the OC, GSH levels in the untreated and 5-hour HBN lenses (Fig. 3A) were similar, indicating that high pressure did not affect GSH levels. As a result of 5-hour HBO exposure, the levels of GSH were significantly depleted (2.6-fold; P < 0.0001) compared with GSH levels from 5-hour HBN lenses. Extending the HBN exposure time to 15 hours results in a slight decrease in GSH levels relative to 5-hour HBN lenses; however, in the presence of HBO, the levels of GSH are significantly reduced (3.5-fold; P < 0.0001) relative to 15-hour HBN lenses. Moreover, GSH levels in 15-hour HBO lenses are more depleted relative to 5-hour HBO lenses (1.7-fold, P < 0.01), indicating that increased exposure time to HBO produced a further reduction in GSH levels.

In the IC, GSH levels between untreated and 5-hour HBN lenses were similar but the concentration of GSH was reduced to almost half that measured in the OC (Fig. 3A). This is consistent with the natural gradient for GSH with levels higher in the OC relative to the IC.²⁰ As a result of 5-hour HBO treatment, GSH levels were significantly reduced (3.5-fold; P < 0.0001) relative to 5-hour HBN lenses. In 15-hour HBN lenses, GSH levels were slightly decreased relative to 5-hour HBN lenses; however, in 15-hour HBO lenses, the levels of GSH were notably reduced (3.6-fold, P < 0.01) relative to 15-hour HBN lenses. In addition, GSH levels were significantly depleted in 15-hour HBO lenses compared with 5-hour HBO lenses (1.5-fold; P < 0.01).

Finally, in the core, GSH levels were lowest in both untreated and 5-hour HBN lenses compared with the other regions. There was a significant decrease in GSH levels in 5-hour HBO lenses compared with 5-hour HBN lenses (3.5-fold; P < 0.0001) and a further depletion of GSH in 15-hour HBO lenses compared with 15-hour HBN lenses (6.1-fold; P < 0.0001). The decrease in GSH was greatest in the core relative to the OC and IC regions. Because depletion of GSH in the core relative to the cortex is a key feature in the formation of ARN cataracts, it appears that by exposure of bovine lenses to HBO for 15 hours, we are able to initiate one of the key processes involved in cataractogenesis in humans.

High levels of GSH are maintained by an active GSH redox system in which oxidized GSH (GSSG) is rapidly reduced to GSH by GSH reductase. As a result of oxidative stress, the ability of GSH reductase to regenerate GSH becomes less efficient and as a result, GSSG accumulation is often observed.²⁸ To determine if this was the case with exposure of lenses to HBO, we measured GSSG concentrations in the different regions of untreated and hyperbaric gas-treated lenses (Fig. 3B). In the OC, GSSG concentrations in untreated lenses and 5-hour HBN lenses were very similar and slightly higher than levels measured in the IC and core regions.

In 5-hour HBO lenses, the GSSG concentrations were similar to 5-hour HBN lenses. Extending the HBO exposure

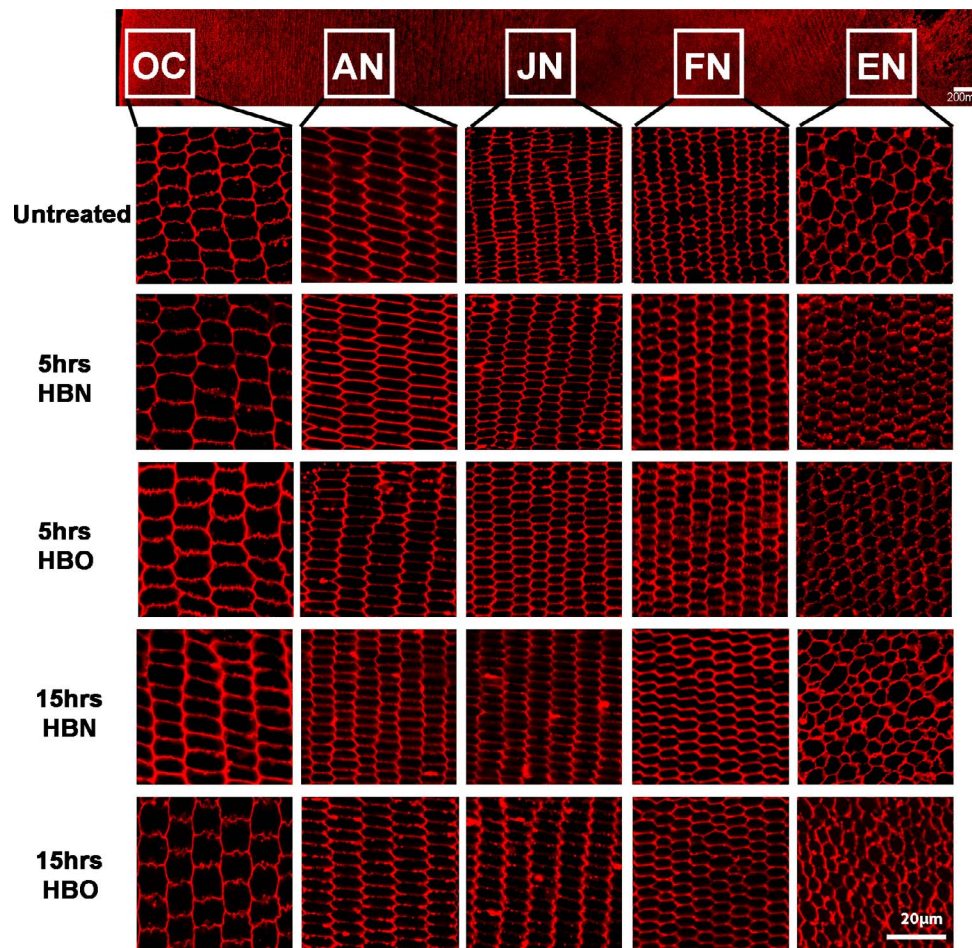


FIGURE 2. Effect of HBN and HBO exposure on fiber cell morphology in bovine lenses. Montage of extended confocal images from an equatorial cryosection from an untreated bovine lens labeled with the membrane marker WGA (red) extending from the capsule to the EN (core) region. The boxes indicate the areas from which high-magnification images were taken. Scale bar: 200 μ m. The high-magnification images displayed are representative images captured from the OC, AN, JN, FN, and EN of untreated lenses (analyzed immediately after dissection), 5-hour HBN, 5-hour HBO, 15-hour HBN, or 15-hour HBO lenses. Scale bar: 20 μ m.

time to 15 hours resulted in a depletion of GSSG levels relative to 15-hour HBN and 5-hour HBO lenses, although this depletion was only significant when compared with 5-hour HBO lenses (2.6-fold; $P < 0.05$). In the IC, GSSG levels were similar between fresh and 5-hour HBN lenses; however, GSSG levels were significantly reduced following 5-hour HBO treatment compared with 5-hour HBN treatment (3.2-fold, $P < 0.01$). A similar depletion was also evident in 15-hour HBO lenses relative to 15-hour HBN lenses (2.4-fold; $P < 0.01$). In the core, GSSG levels were low, with significant reductions evident between 5-hour HBN and 5-hour HBO lenses (2.4-fold, $P < 0.01$) and 15-hour HBN and 15-hour HBO lenses (21-fold; $P < 0.01$).

Lipid Peroxidation (MDA). Because lipid peroxidation is a well-established marker of oxidative stress, we next measured levels of a major by-product of lipid peroxidation, MDA, in the different regions of untreated and hyperbaric-treated lenses (Fig. 4). In the OC, untreated and 5-hour HBN lenses exhibited relatively low levels of MDA; however, after 5 hours of HBO exposure, MDA levels were significantly increased relative to 5-hour HBN lenses (2.3-fold, $P < 0.0001$). In 15-hour HBN lenses, the levels of MDA were slightly decreased relative to the fresh and 5-hour HBN controls. However, in 15-hour HBO lenses, the MDA levels in this group were significantly increased relative to 15-hour

HBN lenses (3.9-fold, $P < 0.0001$). Interestingly, despite the longer exposure to oxygen, the levels of MDA in 15-hour HBO lenses were not significantly increased compared with the MDA levels in 5-hour HBO lenses.

A similar trend was evident in the IC and core. Malondialdehyde levels were significantly increased as a result of 5-hour HBO exposure in the IC (8.2-fold, $P < 0.0001$) and core (2.7-fold, $P < 0.0001$) compared with 5-hour HBN controls. Furthermore, increased exposure of HBO from 5 to 15 hours did not result in a further increase in MDA levels in the IC or core. However, the MDA levels were highest in the core relative to the OC and IC regions and were approximately 2.6-fold greater than the MDA levels in the core of nitrogen controls. Taken together, it appears that exposure of lenses to oxygen results in increased MDA levels relative to controls, with MDA concentrations highest in the core regions following HBO treatment. This indicates that the lens core is particularly susceptible to oxidative damage.

Collectively, these findings demonstrate that exposure to HBO for 15 hours results in depleted GSH levels and increased MDA levels, particularly in the lens core, which is consistent with early biochemical changes that are known to precede human nuclear cataract formation.

Mixed Disulfide Formation. The depletion of GSSG levels led us to investigate whether GSSG was involved in PSSG

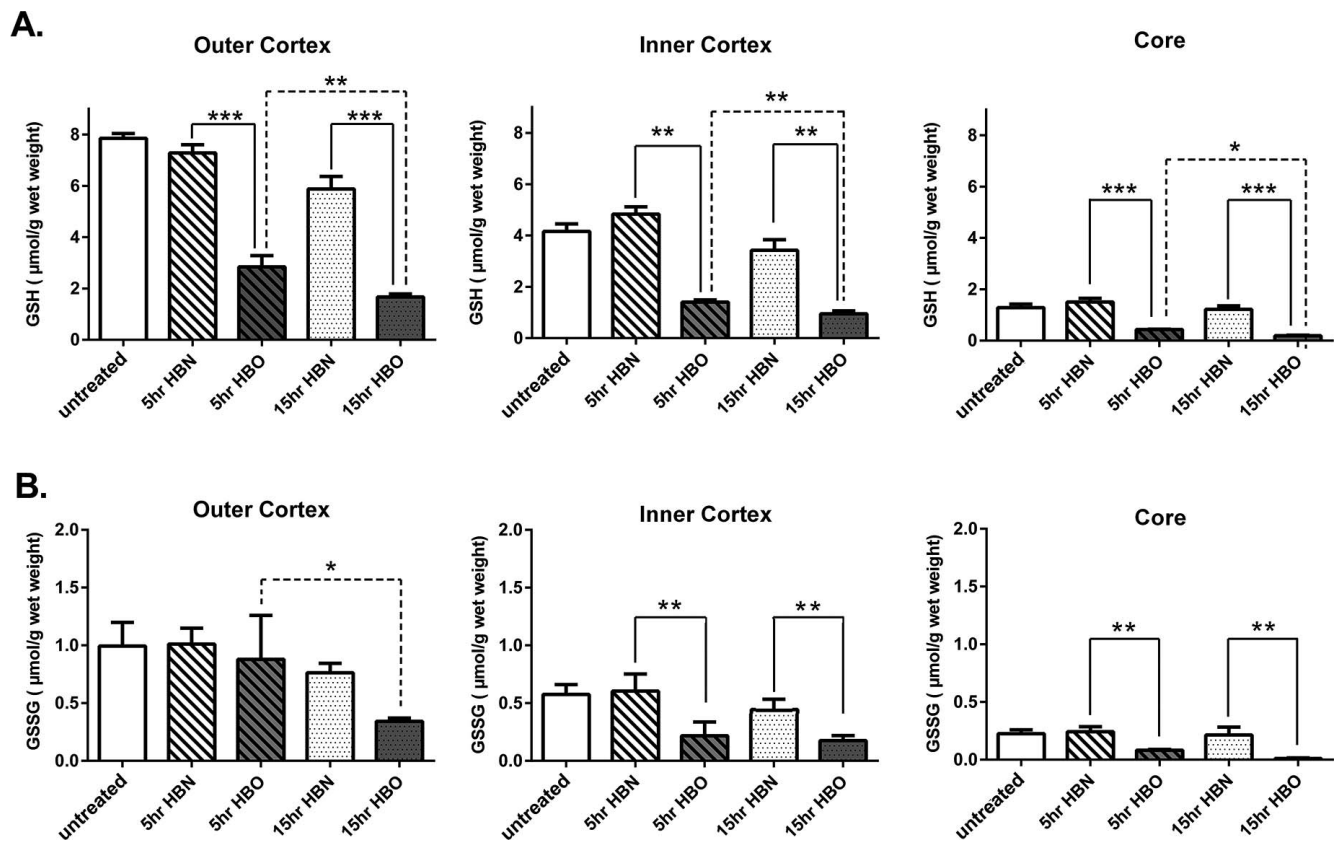


FIGURE 3. Effect of HBO treatment on GSH/GSSG levels in the different regions of the bovine lens. Untreated lenses (analyzed immediately after dissection), 5-hour HBN, 5-hour HBO, 15-hour HBN, or 15-hour HBO-treated lenses were dissected into the OC, IC, and core. (A) Glutathione or (B) GSSG levels were measured and results expressed as mean ± SEM with *n* = 5 lenses per group. For GSH: **P* < 0.05, ***P* < 0.01, ****P* < 0.0001. For GSSG: **P* < 0.05, ***P* < 0.01.

(protein mixed disulfide) formation under HBO conditions. Although PSSGs are present in normal clear lenses,²⁹ it has been reported that there is a profound increase in PSSG formation with advancing age, on exposure to prolonged oxidative stress,^{29,30} and in human ARN cataract.³¹ To investigate this, Western blot analysis was performed using a specific anti-GSH antibody to examine the levels of total PSSG in samples prepared from the WS and US fractions of lenses treated for 5 hours or 15 hours in the presence of either HBN or HBO. The US samples showed more PSSG staining at higher molecular weights compared with the WS samples. For this reason, only the US protein fraction is reported.

With 5-hour HBN treatment, a number of PSSG bands were detected in the OC and IC at 37, 50, 58, and approximately 250 kDa (Fig. 5A, left panel) with no PSSG bands detected in the core (Fig. 5A, left panel). With 5-hour HBO treatment, additional bands at 15, 60 to 70, 90, and 100 to 150 kDa (highlighted by the arrows) in the OC and IC regions were detected (Fig. 5A, right panel), and a significant increase in the intensity of the total levels of PSSG (Fig. 5C) in the OC and IC was measured as a result of HBO exposure. Exposure to 15-hour HBN showed a similar pattern to that of the 5-hour HBN-treated lenses, except that bands became apparent in the core (Fig. 5B, left panel). These bands were also evident after 15-

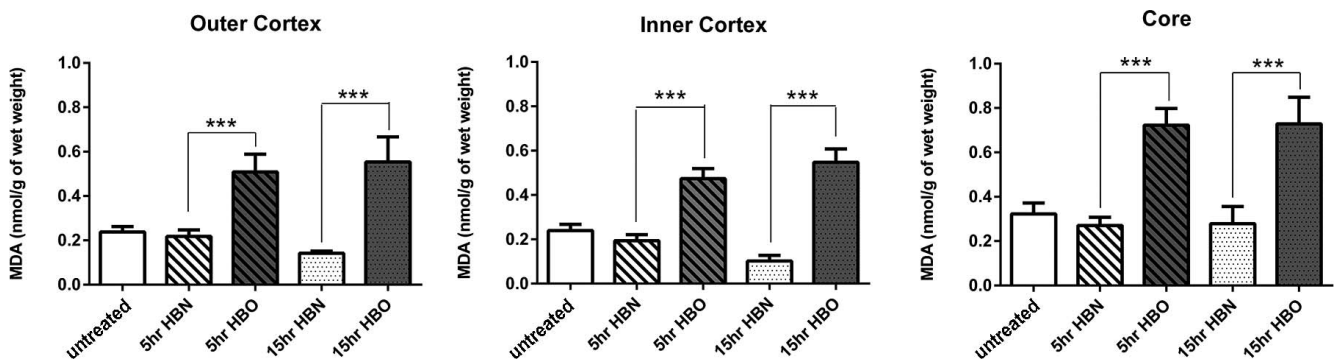


FIGURE 4. Effect of HBO on the levels of the lipid peroxidation marker MDA in different regions of the bovine lens. Untreated lenses (analyzed immediately after dissection), 5-hour HBN, 5-hour HBO, 15-hour HBN, or 15-hour HBO-treated lenses were dissected into the OC, IC, and core. Malondialdehyde levels were measured and results expressed as mean ± SEM with *n* = 5 lenses per group. ****P* < 0.0001.

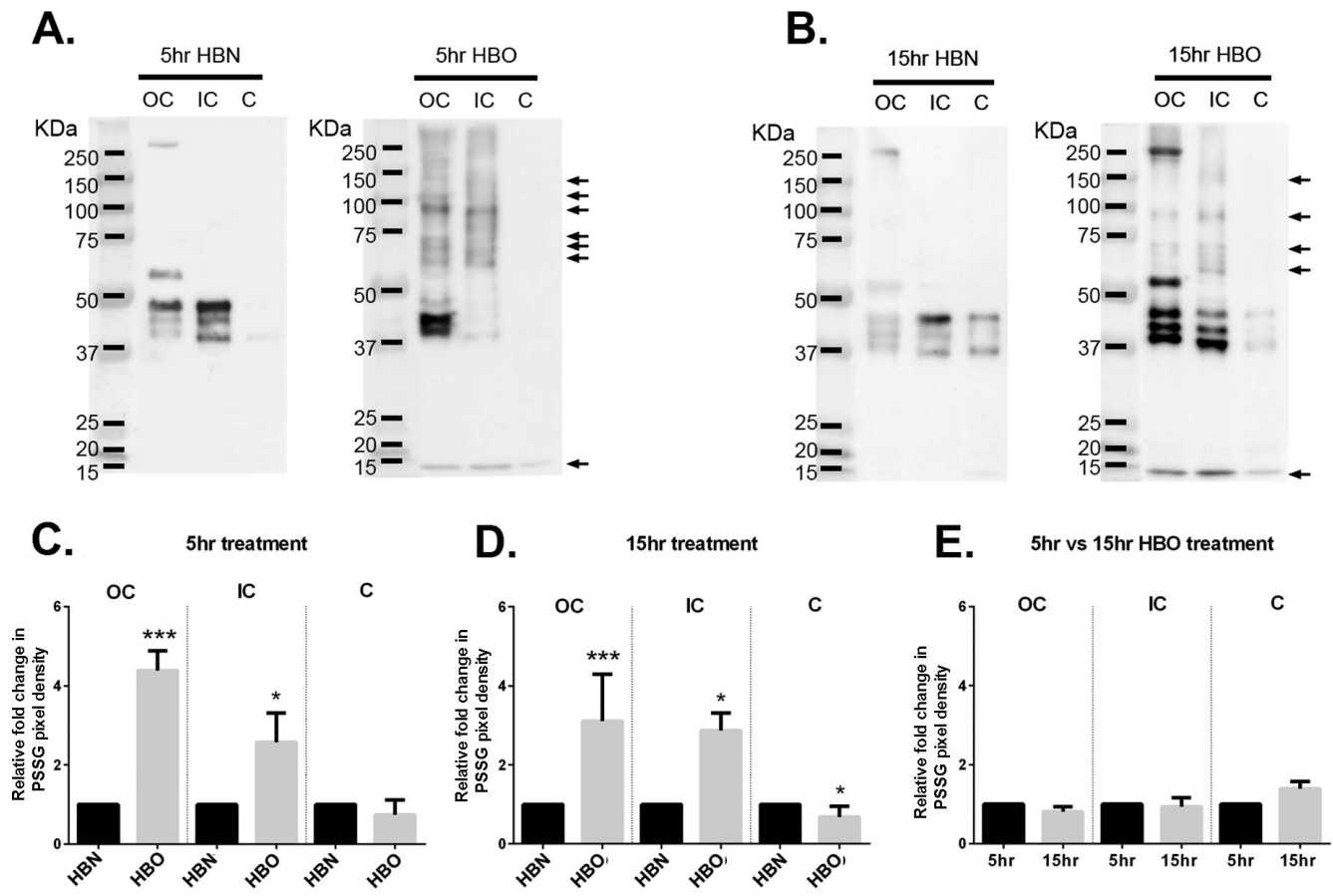


FIGURE 5. Effects of HBO on PSSG formation. Urea-soluble fractions from the OC, IC, and core regions of (A) 5-hour HBN or HBO-treated lenses or (B) 15-hour HBN or HBO-treated lenses were analyzed by Western blot for the level of glutathionylated proteins using an anti-GSH antibody. (A, B) Representative immunoblots are shown, with *arrows* representing additional bands that are detected as a result of HBO treatment but not HBN treatment. (C, D) Pixel density of all PSSGs (between 15 and 250 kDa) as a result of exposure to HBO at 5 hours or 15 hours, and in comparison with the value of the 5-hour HBN-treated lenses (C) or 15-hour HBN-treated lenses (D), each normalized to 1. (E) Pixel density of all PSSGs as a result of 15-hour HBO exposure, and in comparison with the value of the 5-hour HBO-treated lenses (normalized to 1); 15 μ g protein was loaded per lane, and equal loading was confirmed by probing with a β -actin antibody (data not shown). The data are expressed as mean \pm SD with $n = 6$ lenses, * $P < 0.05$, *** $P < 0.001$.

hour HBO exposure (Fig. 5B, right panel). With 15-hour HBO treatment, additional bands (highlighted by the arrows) appeared at 15, 60 to 70, 90, and 150 kDa in the OC and IC (Fig. 5B, right panel) that were not present at 15-hour HBN treatment (Fig. 5B, left panel). In addition, the intensity of total PSSG bands was enhanced in these regions as a result of HBO treatment compared with HBN treatment (Fig. 5D). Finally, we compared the total density of PSSG bands between 5-hour and 15-hour HBO lenses (Fig. 5E). We found no significant increase in PSSG density as a result of longer exposure times to HBO in the OC, IC, and core regions.

Overall, it appears that as a result of HBO treatment, there is an increase in PSSG formation in the cortex, but not the core of 5-hour HBO-treated lenses (relative to 5-hour HBN lenses). Increasing the time of exposure of HBO treatment led to the appearance of PSSG bands in the core, but these bands were also evident in the 15-hour HBN group. Finally, extending HBO treatment from 5 to 15 hours did not appear to result in a further increase in the number or intensity of PSSG bands in the cortex.

Protein Aggregation. If glutathionylated proteins are not reduced, oxidative stress will lead to conformational protein changes that induce PSSP formation and HMW aggregate complexes. To investigate this, samples of WS and US protein fractions from lenses treated for 5 hours or 15 hours in HBN or

HBO were used for SDS-PAGE analysis to visualize the presence of HMW bands at the top of the separating gel following staining with Coomassie Blue (Fig. 6). In the WS samples (Fig. 6A), a higher oligomer band (see arrow) was observed in the core of the 5-hour HBO lenses; however, this band was also evident in the HBN group (see arrow). A similar finding was also apparent in the WS samples of 15-hour HBN and HBO lenses (see arrows). Interestingly, an approximately 55 kDa broad band was seen in the IC of 15-hour HBO-treated lenses that disappeared under reducing conditions (data not shown), indicating possible disulfide crosslinking of a crystallin. In the US samples (Fig. 6B) from 5-hour HBO lenses, a higher molecular-weight band (see arrow) was detected in the OC, which was also present in 5-hour HBN lenses (see arrow). The same sized band was also evident in the US samples of the 15-hour treatment groups (see arrows). Overall, these findings indicate that the treatment of lenses with high-pressure oxygen for up to 15 hours does not result in the formation of HMW aggregates.

Collectively, these results show that depletion of GSSG may be a consequence of increased PSSG formation, although we cannot rule out the possibility of GSSG leakage from the lens.³² However, increased PSSG formation was detected only in the cortical regions and not the core. Furthermore, we were not able to detect HMW aggregates, indicating that our model was

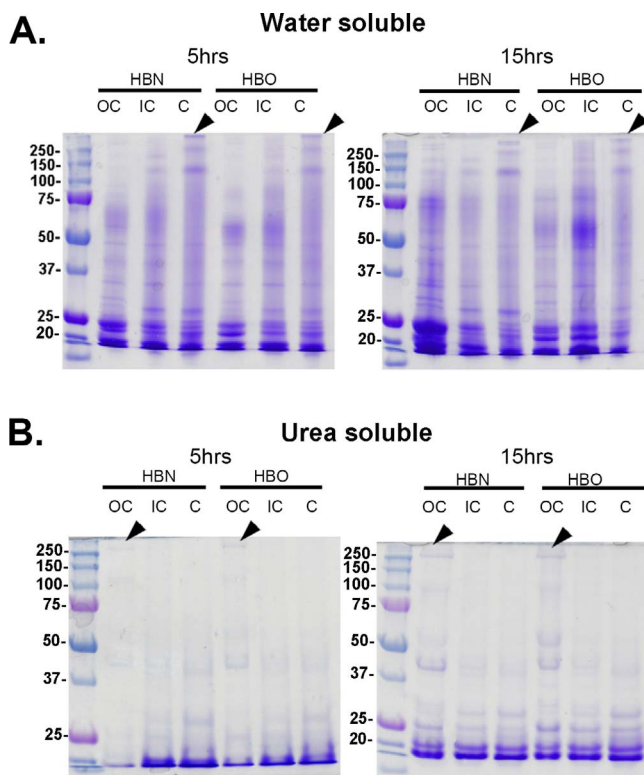


FIGURE 6. Effects of HBO on HMW protein aggregate formation. Approximately 15 μ g of nonreduced WS (A) or US proteins (B) were electrophoresed and then stained with Coomassie Blue to identify HMW protein aggregates. *Arrowheads* indicate the presence of HMW protein aggregates (molecular weight >250 kDa) that were apparent in the WS and US fractions of HBN- and HBO-treated lenses.

able to initiate some, but not all of the early biochemical changes known to precede human nuclear cataract.

Effects of HBO Exposure on Optical Properties of the Lens

Having established that some changes of the biomarkers of ARN cataract are apparent at the biochemical level as a result of HBO treatment, we next wanted to determine whether these changes altered the key parameters of lens geometry and refractive index that determine the optical properties of the lens, and how these changes affect overall vision quality.

Lens Geometry. To measure the effects of HBO exposure on overall lens geometry, we used high-resolution T2-weighted image datasets (Fig. 7A), and extracted measurements of key parameters that determine lens geometry, namely, axial thicknesses (T_{a-p}), equatorial radius (R_c), and the radii and conic factors of the anterior (R_a , Q_a) and posterior (R_p , Q_p) surfaces (Fig. 7B), from untreated lenses and HBN- and HBO-treated lenses organ cultured for either 5 hours or 15 hours. There were no significant differences between any of the measured parameters of the untreated and HBN and HBO lenses cultured for 5 hours; however, there was a difference in the axial thickness and anterior and posterior radii parameters of HBO lenses cultured for 15 hours relative to the untreated HBN lenses. Although not statistically significant, the decrease in axial thickness and larger radii of curvature indicate that 15-hour HBO-treated lenses may be thinner and flatter relative to the other lenses. To visualize changes in lens geometry, the extracted parameters for each condition were then averaged

and used to reconstruct the shape of the lens (Fig. 7C). Again, no significant changes were evident in the 15-hour HBO lenses relative to 15-hour HBN lenses; however, there appeared to be a trend toward thinning and flattening of HBO-treated lenses.

Refractive Index. T2 constant maps that provide a measure of the water-to-protein ratio, from which the GRIN can be calculated,¹⁶ were obtained for bovine lenses organ cultured in AAH for 5 hours or 15 hours (untreated lenses), 5-hour HBN/HBO lenses, or 15-hour HBN/HBO lenses (Fig. 8A). It can be seen that for 5-hour HBN- or HBO-treated lenses, there were no significant differences between these T2 constant maps (Fig. 8A, left panel). However at 15 hours, the HBO-treated lenses showed a different T2 constant pattern compared with the 15-hour HBN group (Fig. 8A, right panel). Equatorial plots of these T2 constant maps were extracted and plotted against relative distance into the lens (r/a), where 0 represent the lens core and 1 represents the lens periphery (Fig. 8B). Here it was apparent that there was no significant difference among the three treatment groups at 5 hours (Fig. 8B, left panel). However, a significant increase of T2 values was observed in the core of HBO-treated lenses at 15 hours relative to both the untreated (15-hour cultured) and HBN-treated lenses (Fig. 8B, right panel). Because T2 constants are inversely proportional to refractive index, GRIN profiles were calculated from the estimated T2 maps (Fig. 8C). Here it can be seen that there were no changes in the GRIN profile between the HBN- and HBO-treated lenses after 5 hours (Fig. 8C, left panel), but there was a significant decrease in the refractive index of the core of lenses exposed to HBO for 15 hours (Fig. 8C, right panel). Equatorial profiles of these GRIN maps were extracted and superimposed (Fig. 8D), with no noticeable change of GRIN evident at 5 hours between treatment groups (Fig. 8D, left panel), and with GRIN profiles similar to that reported previously for bovine lenses.³⁵ However, the refractive index of lenses exposed to HBO for 15 hours was lower in the core when compared with the untreated and HBN-treated lenses (Fig. 8D, right panel). Taken together, it appears that HBO treatment of lenses for 15 hours produces a change in the water/protein ratio and therefore the GRIN, which when combined with the trend toward lens thinning (Fig. 7) would suggest that the optical properties of lenses exposed to HBO for 15 hours may be altered.

Modeling Lens Optical Power and Vision Quality. The geometrical parameters (Fig. 7) and GRIN profiles (Fig. 8) extracted from untreated (5-hour/15-hour cultured), 5-hour HBN/HBO lenses, and 15-hour HBN/HBO lenses were implemented in ZEMAX to calculate the lens optical power (Fig. 9A). Consistent with our findings of a trend toward a thinner lens (Fig. 7B) and significantly decreased GRIN profile in the core (Fig. 8D) of lenses exposed to 15 hours of HBO, a significant reduction of optical power was apparent only in the 15-hour HBO treatment group (Fig. 9A). To assess how changes in the GRIN and geometry induced by culturing lenses in HBO for 15 hours specifically affects overall vision quality, we used an anatomically accurate ZEMAX model of the bovine eye created in an earlier study.¹⁶ Model simulations were initially performed to calculate the optimal focal length of the model eye. In these simulations, the vitreous chamber length ($V_T = 12.8$ mm) was allowed to vary between the different conditions to determine the focal length of the model eye that provides the optimal focus. Using this approach, it is apparent that untreated and HBN-treated lenses cultured for up to 15 hours and HBO-treated lenses cultured for 5 hours have optimal focal lengths that are not significantly different from the vitreous chamber length (12.8 mm) measured in the bovine eye (Fig. 9B). However, 15-hour HBO lenses exhibited a significant increase in the optimal focal length that would result in images being focused behind the retina, indicating that exposure to

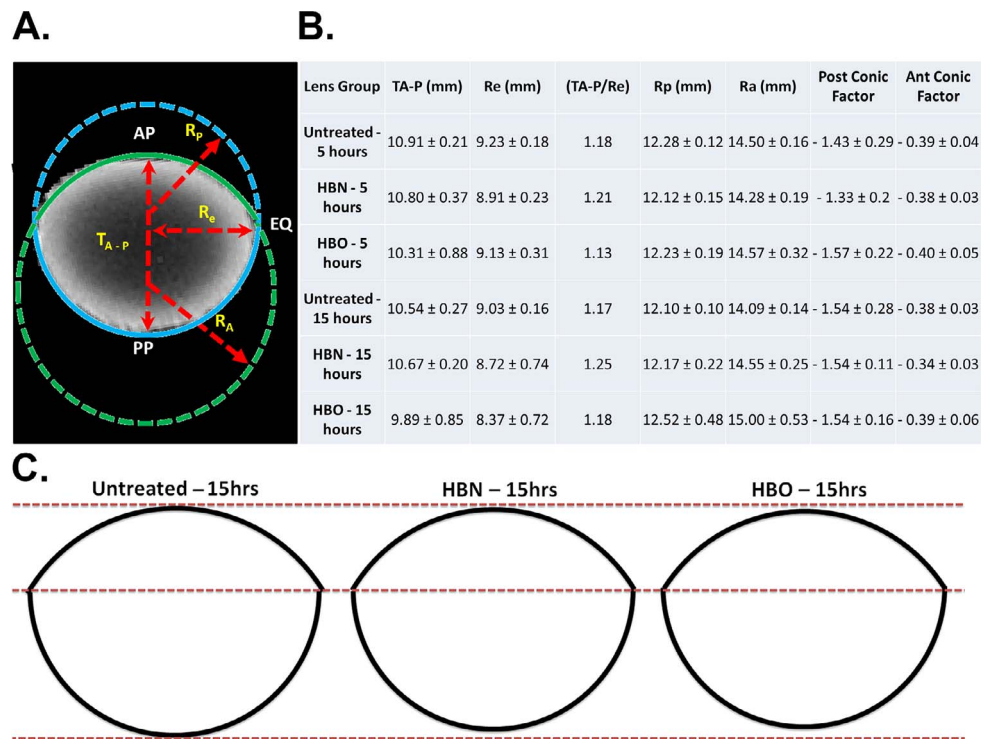


FIGURE 7. Effects of HBO exposure on lens geometry. (A) Representative high-resolution T2-weighted image of the bovine lens captured with MRI showing the anterior pole (AP), posterior pole (PP), equator (EQ), front (R_a), and back (R_p) radii of curvature, the equatorial radius (R_e) and axial thickness (T_{A-P}), which were extracted from the image by using a MATLAB custom-written program. (B) Table summarizing the average values extracted for geometrical parameters defined in (A) plus the anterior and posterior conic factors extracted from MRIs of lenses organ cultured in all the experimental groups. (C) The average values for these lens surface radii, conic factor, and thicknesses listed in (B) have been used to draw representative profiles for lenses organ cultured in either the absence or presence of either HBN or HBO at 15 hours. Note: the term “untreated” here refers to lenses cultured in AAH for 5 hours or 15 hours without exposure to HBN or HBO.

HBO is causing a hyperopic shift. In addition to measurements of optical power, the ZEMAX software also quantifies the Seidel aberrations (coma, astigmatism, distortion, field curvature, longitudinal chromatic, and transverse chromatic) that are associated with the passage of light through an optical system. We found no significant changes in estimated Seidel aberration levels in the lenses of each of the different groups, including the 15-hour HBO-treated lenses (data not shown), which is consistent with the clarity of these lenses observed in Figure 1. Finally, to visually assess what effects the changes in lens optical power have on overall image quality of the bovine eye, we used the Image Simulation capability of ZEMAX to determine the ability of the model eye to reproduce an input image (Fig. 9C). This analysis was performed using either the calculated optimal focal length (17.5 mm) for the model eye, or a fixed focal length given by the vitreous chamber depth (12.8 mm), which more closely represents the situation in the *in vivo* bovine eye. Analysis performed using the calculated optimal focal length showed that image quality is unaffected for the different lens groups (Fig. 9C, left column). However, the same analysis performed using the vitreous chamber depth as a “fixed” focal length for each group revealed a blurring of the image for lenses exposed to HBO for 15 hours (Fig. 9C, right column), consistent with the observed hyperopic shift in this treatment group (Fig. 9B). Overall, this confirms that the nature of the 15-hour HBO-induced optical deficiency was a hyperopic shift.

In summary, these MRI studies show that longer exposure of lenses to HBO results in changes to the optical properties of

the lens that would compromise vision quality produced by the bovine eye.

DISCUSSION

This study was designed to assess the morphologic, biochemical, and optical changes brought about by exposure of bovine lenses to HBO and to determine whether this would be a suitable *in vitro* model for mimicking nuclear cataract formation in humans. From our analysis, it appears that with short (5-hour) or long (15-hour) HBO treatment, biochemical changes were induced that were consistent with the early changes that precede nuclear cataract formation. These changes, most notably in the core region of the lens, include depletion of GSH and an increase in the oxidative stress marker MDA. We also found that GSSG levels were depleted in all regions of the lens. We should point out that in the untreated and nitrogen control lenses, GSH levels were lower and GSSG levels higher than previously reported,^{14,34} suggesting that there may have been some artifactual oxidation of GSH during the assay process. However, given that all of our samples were processed in the same way, we feel that GSH and GSSG levels are comparable among the three groups. The depletion of GSSG following HBO treatment coincides with an increase in PSSG formation in the cortical regions of the lens, but not the core. There was also a lack of HMW aggregates, consistent with the transparent appearance of these lenses, even after long periods of exposure to HBO. Although biochemical changes, such as GSH depletion, were evident following 5-hour HBO treatment, optical changes were detectable only after exposure

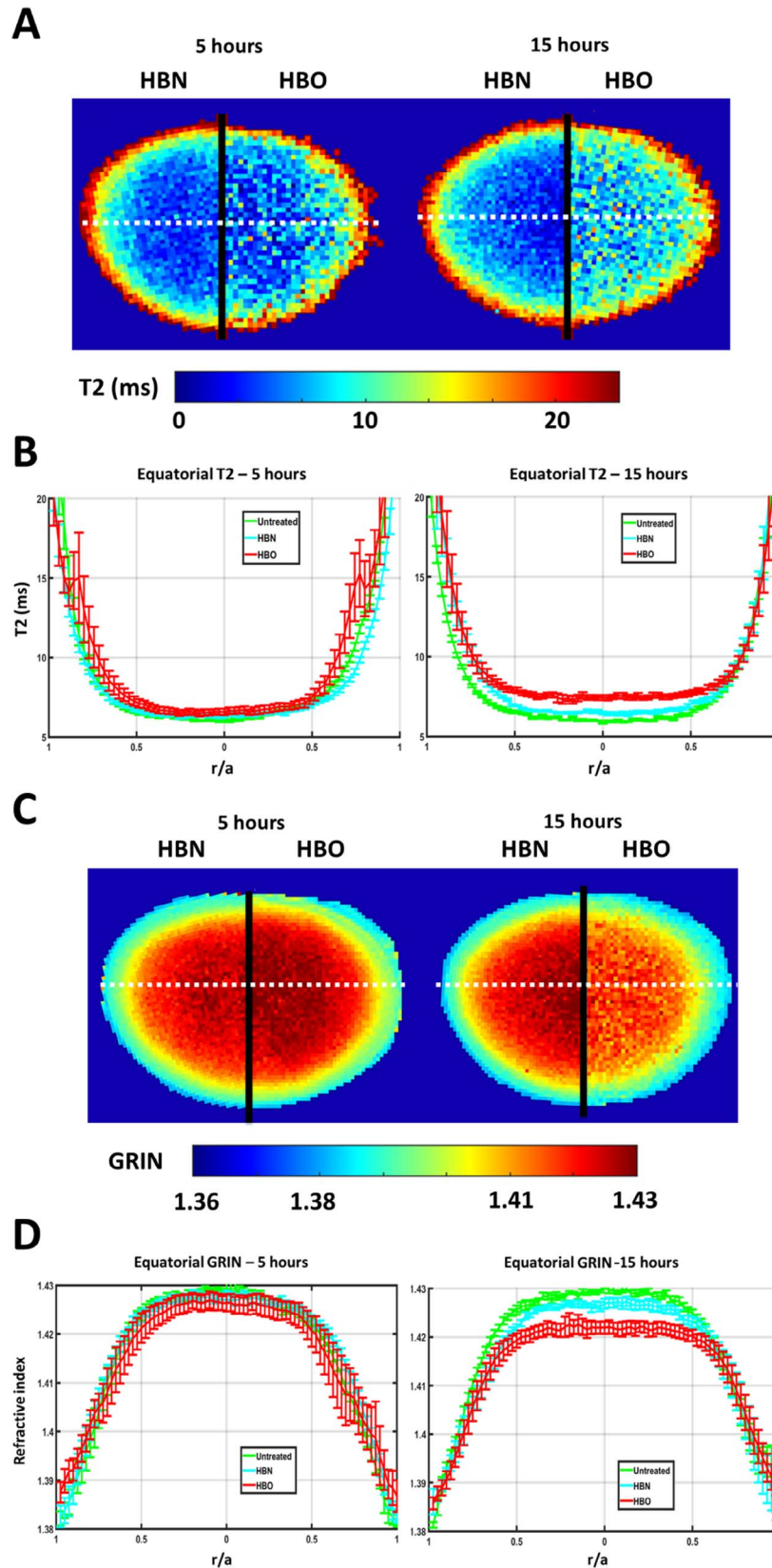


FIGURE 8. Effect of HBO exposure on the GRIN in the bovine lens. (A) Maps of T2 constants calculated from lenses treated with HBN or HBO for 5 hours (*left*) or 15 hours (*right*). The numbers on the *color bar* represent T2 values in milliseconds. (B) Line profiles of T2 constants extracted through the equatorial axis of untreated lenses (*green*), HBN (*blue*), or HBO (*red*) for 5 hours (*left*) or 15 hours (*right*) are plotted against the relative distance into the lens (r/a). (C) T2 constant maps obtained for lenses treated with HBN or HBO for 5 hours (*left*) or 15 hours (*right*) shown in (A) have been converted into *color-coded maps* of refractive index to visualize the GRIN. (D) Line profiles of refractive index extracted through the equatorial axis of untreated lenses (*green*), HBN (*blue*), or HBO (*red*) for 5 hours (*left*) or 15 hours (*right*) are plotted against the relative distance into the lens (r/a).

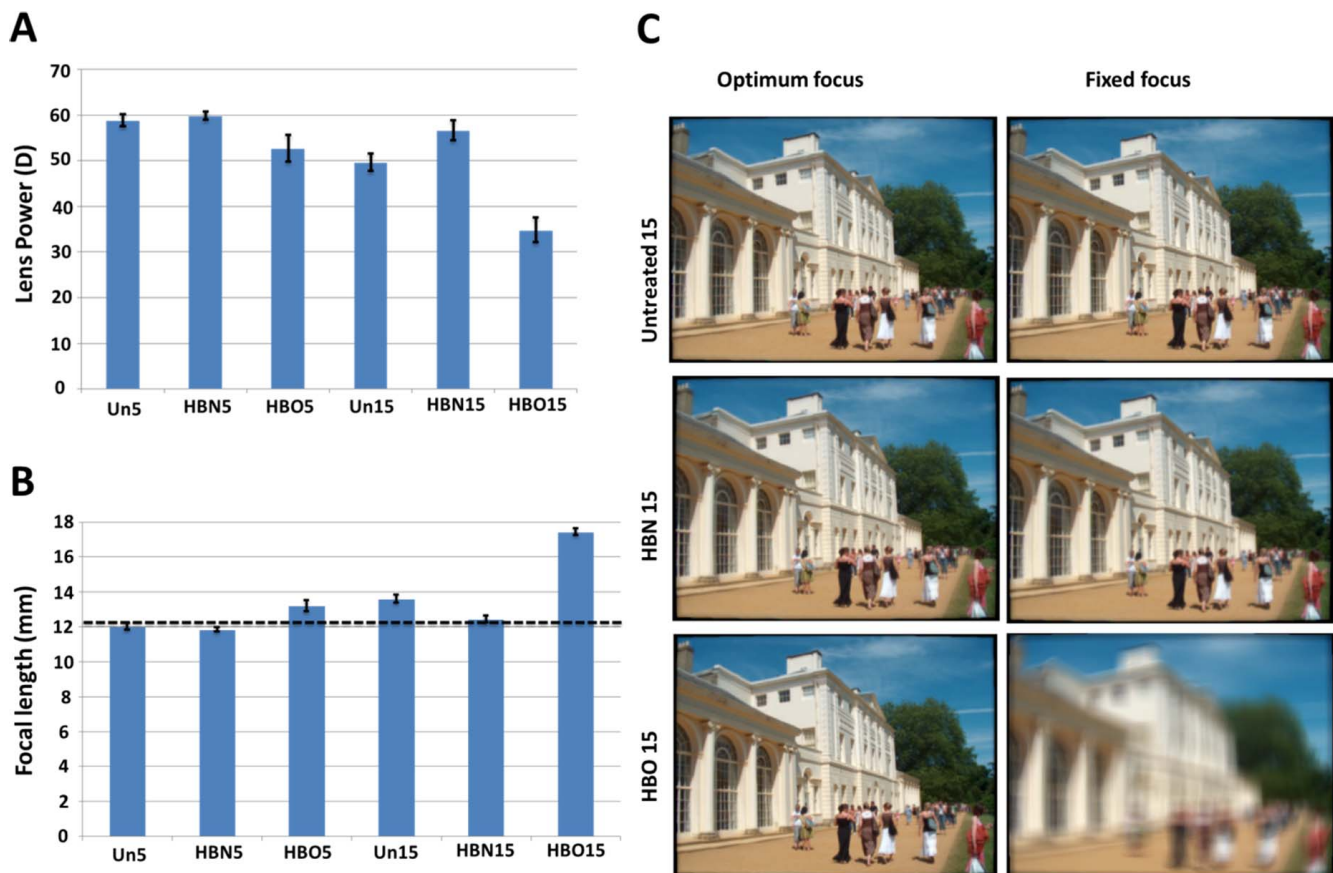


FIGURE 9. Effect of HBO on the optical properties of the bovine lens and vision quality in a model of the bovine eye. **(A)** The geometric parameters (Fig. 7) and GRIN profiles (Fig. 8) were inputted into ZEMAX to calculate the lens power in diopters for each experimental treatment group. **(B)** The optimal focal length calculated by using the “best focus” feature of the ZEMAX modeling platform that calculates for each lens dataset the ideal focal length of a model bovine eye developed in a previous study.¹⁶ **(C)** The ability of the model bovine eye to reproduce an input image of a scene was tested by using the Image Simulation of ZEMAX. This analysis was performed for each treatment group using either the optimal focal length calculated by ZEMAX (*left column*) or a fixed focal length (*right column*) that was set to the vitreous chamber depth of 12.8 mm (*dotted line*) measured in the bovine eye.

to HBO for 15 hours. These included a decrease in the refractive index of the lens core, a trend toward reduced lens thickness, and an increase in optimal focal length consistent with a hyperopic shift commonly seen in elderly patients. Collectively, our findings suggest that HBO treatment of bovine lenses results in changes that are consistent with the aging process and that this bovine model may be useful as a model of accelerated aging, but not necessarily as a model of ARN cataract.

There were some interesting findings from our study that we feel warrant further discussion.

Human studies clearly demonstrate that with increasing age, PSSG formation increases in the lens center.²⁹ In addition, increased PSSG formation also has been detected in the core of older guinea pigs treated with HBO,⁹ and in the core of bovine lenses treated with HBO.¹⁴ Therefore, it was surprising that in contrast to these studies, we were able to detect increased PSSG formation only in the cortical regions, but not the core region of HBO-treated bovine lenses. We have a couple of suggestions that might explain these results. First, increased PSSG formation in the cortex may represent an early event in the aging process. Longer treatment times with HBO may exacerbate the aging/cataractogenic process with PSSG formation in the core becoming apparent. Second, our Western blot method relies on an antibody approach that recognizes GSH

protein complexes. Previously, other research groups have used more sensitive methods such as HPLC and mass spectrometry to identify specific protein targets of glutathionylation in the lens core as a result of HBO treatment. These glutathionylated proteins include β - and γ -crystallins^{15,35} and cytoskeletal proteins, such as β -actin, vimentin, and tubulin.³⁶ In the future, these tools could be applied to examining the core of HBO-treated lenses to verify our Western blot findings, as well as identify specific proteins modified by GSH in the lens cortex. Third, we also should consider that cysteine mixed protein disulfide (PSSC) formation rather than PSSG formation may be the major protein mixed disulfide formed in the lens core of HBO-treated bovine lenses. Bovine lenses contain relatively equal amounts of PSSG to PSSC, whereas the typical ratio of PSSG/PSSC is 5.5:1.0 in human lenses, 7.6:1.0 in rabbit lenses, and 17.0:1.0 in guinea pig lenses.^{29,30} In addition, the distribution of protein mixed disulfides in the cortex versus nucleus is different among species.³⁰ For example, in rat lenses, most PSSGs are located in the cortex and PSSCs in the core, whereas in human lenses, PSSG and PSSC almost always have a preferential presence in the core.³⁰ With this in mind, further work is required to determine the relative amounts and distribution of PSSG and PSSCs in the bovine lens in the absence and presence of HBO.

Another interesting finding to emerge from our study was that HBO treatment of bovine lenses for 15 hours resulted in changes in the water/protein ratio specifically in the lens IC and core, resulting in a decrease in the GRIN relative to control lenses. This is a similar finding to what has been shown in the core of aged human lenses.³⁴ At this stage, it is unknown if the decrease in GRIN in the core of the HBO lenses is due to a decrease in protein content or an increase in water content; however, an earlier study using Raman micro-spectroscopy has shown that in human lenses water content increases with age.³⁵ Such an increase in water content would account for the observed gradual hyperopic shift that is observed with advancing age,^{37,38} and that is distinctly different from the abrupt myopic shift that is a clinical precursor for the onset of lens cataract.^{8,39,40} Our in vitro HBO model appears to mimic optical changes associated with accelerated aging rather than cataract formation per se. However, it is important to note that in vivo HBO exposure of 30 to 35 treatments over a 3-month period in 16- to 17-month-old guinea pigs eventually induces a reversible myopic shift⁴¹ that is a precursor of cataract development. Whether the sequence of myopic shift and cataract formation can be replicated in our in vitro model will be something of interest to examine in the future.

Although the underlying cellular mechanisms that contribute to increased water content observed in the aging human lens, and more specifically in the lens center of the HBO-treated lenses used in this current study, are unknown, it is interesting to note that our laboratory has recently shown that inhibiting the lens circulation system by either pharmacologically blocking Na⁺ pump activity with ouabain, or depolarizing the lens potential by incubating lenses in high extracellular K⁺, also altered the optical properties of the lens.¹⁶ However, in these more targeted experimental perturbations, a myopic shift in lens optical power was observed rather than the hyperopic shift observed for HBO-treated lenses in this present study. Taken together, the two studies show that the alteration of specific components of the cellular physiology of the lens that drives the circulation system can either increase (myopic shift) or decrease (hyperopic shift) the optical power of the lens, suggesting the optical properties of the lens are linked to the magnitude of the circulating ion and water fluxes. With regard to how the oxidative stress induced by HBO exposure is causing a change in the refractive index specifically in the lens center, we can envisage at least two scenarios that might account for the observed change: oxidative damage to gap junction channels that decreases cell-to-cell coupling that reduces the outflow of water from the lens core,⁴² and/or changes to protein conformation in the lens core that release water bound to protein to increase the free water content in this region of the lens.⁴³ Further work will be required to distinguish between these two possibilities.

In conclusion, we have shown that exposure of lenses to HBO results in depletion of GSH and increased markers of lipid peroxidation in the lens core, plus an increase in PSSG formation in the lens cortex. These biochemical changes are detected during short HBO exposure and could be used as early indicators of cataract formation. Longer HBO exposure induces additional changes to the water/protein ratio in the lens center and concomitant changes to the optical power of the lens that produces a hyperopic shift in visual acuity. Because a hyperopic shift is observed as a function of aging,^{37,38} our findings indicate that acute HBO exposure has effectively accelerated the aging of these young bovine lenses and suggests that long-term treatment of bovine lenses with HBO may serve as a useful model to study changes that occur in the aging lens.

Acknowledgments

Supported by an Auckland Medical Research Foundation Project Grant, Marsden Fund of New Zealand, Lotteries Health, and a Sir Charles Hercus Health Research Fellowship.

Disclosure: **J.C. Lim**, None; **E. Vaghefi**, None; **B. Li**, None; **M.G. Nye-Wood**, None; **P.J. Donaldson**, None

References

1. World Health Organization. Visual impairment and blindness. Fact sheet N282. May 2009. Available at: <http://www.who.int/mediacentre/factsheets/fs282/en/>. Accessed February 2, 2016.
2. Truscott RJ. Age-related nuclear cataract-oxidation is the key. *Exp Eye Res.* 2005;80:709-725.
3. Lim JC, Umaphathy A, Donaldson PJ. Tools to fight the cataract epidemic: a review of experimental animal models that mimic age related nuclear cataract. [published online ahead of print September 25, 2015]. *Exp Eye Res.* doi:10.1016/j.exer.2015.09.007.
4. Moon RE. Hyperbaric oxygen treatment for decompression sickness. *Undersea Hyperb Med.* 2014;41:151-157.
5. Moon RE. Hyperbaric oxygen treatment for air or gas embolism. *Undersea Hyperb Med.* 2014;41:159-166.
6. Londahl M, Katzman P, Hammarlund C, Nilsson A, Landin-Olsson M. Relationship between ulcer healing after hyperbaric oxygen therapy and transcutaneous oximetry, toe blood pressure and ankle-brachial index in patients with diabetes and chronic foot ulcers. *Diabetologia.* 2011;54:65-68.
7. Londahl M, Katzman P, Nilsson A, Hammarlund C. Hyperbaric oxygen therapy facilitates healing of chronic foot ulcers in patients with diabetes. *Diabetes Care.* 2010;33:998-1003.
8. Palmquist BM, Philipson B, Barr PO. Nuclear cataract and myopia during hyperbaric oxygen therapy. *Br J Ophthalmol.* 1984;68:113-117.
9. Giblin FJ, Padgaonkar VA, Leverenz VR, et al. Nuclear light scattering, disulfide formation and membrane damage in lenses of older guinea pigs treated with hyperbaric oxygen. *Exp Eye Res.* 1995;60:219-235.
10. Borchman D, Giblin FJ, Leverenz VR, et al. Impact of aging and hyperbaric oxygen in vivo on guinea pig lens lipids and nuclear light scatter. *Invest Ophthalmol Vis Sci.* 2000;41:3061-3073.
11. Simpanya ME, Ansari RR, Suh KI, Leverenz VR, Giblin FJ. Aggregation of lens crystallins in an in vivo hyperbaric oxygen guinea pig model of nuclear cataract: dynamic light-scattering and HPLC analysis. *Invest Ophthalmol Vis Sci.* 2005;46:4641-4651.
12. Gosselin ME, Kapustij CJ, Venkateswaran UD, Leverenz VR, Giblin FJ. Raman spectroscopic evidence for nuclear disulfide in isolated lenses of hyperbaric oxygen-treated guinea pigs. *Exp Eye Res.* 2007;84:493-499.
13. Giblin FJ, Schirmscher L, Chakrapani B, Reddy VN. Exposure of rabbit lens to hyperbaric oxygen in vitro: regional effects on GSH level. *Invest Ophthalmol Vis Sci.* 1988;29:1312-1319.
14. Capiello M, Vilardo PG, Cecconi I, et al. Occurrence of glutathione-modified aldose reductase in oxidatively stressed bovine lens. *Biochem Biophys Res Commun.* 1995;207:775-782.
15. Padgaonkar VA, Leverenz VR, Fowler KE, Reddy VN, Giblin FJ. The effects of hyperbaric oxygen on the crystallins of cultured rabbit lenses: a possible catalytic role for copper. *Exp Eye Res.* 2000;71:371-383.
16. Vaghefi E, Kim A, Donaldson PJ. Active maintenance of the gradient of refractive index is required to sustain the optical properties of the lens. *Invest Ophthalmol Vis Sci.* 2015;56:7195-7208.

17. Vaghefi E, Pontre BP, Jacobs MD, Donaldson PJ. Visualizing ocular lens fluid dynamics using MRI: manipulation of steady state water content and water fluxes. *Am J Physiol Regul Integr Comp Physiol*. 2011;301:R335-R342.
18. Birkenfeld J, de Castro A, Marcos S. Contribution of shape and gradient refractive index to the spherical aberration of isolated human lenses. *Invest Ophthalmol Vis Sci*. 2014;55:2599-2607.
19. al-Ghoul KJ, Costello MJ. Light microscopic variation of fiber cell size, shape and ordering in the equatorial plane of bovine and human lenses. *Mol Vis*. 1997;3:2.
20. Giblin FJ. Glutathione: a vital lens antioxidant. *J Ocul Pharmacol Ther*. 2000;16:121-135.
21. Ho E, Karimi Galougahi K, Liu CC, Bhindi R, Figtree GA. Biological markers of oxidative stress: applications to cardiovascular research and practice. *Redox Biol*. 2013;1:483-491.
22. Pierscionek BK, Chan DY, Ennis JP, Smith G, Augusteyn RC. Nondestructive method of constructing three-dimensional gradient index models for crystalline lenses: I. Theory and experiment. *Am J Optom Physiol Opt*. 1988;65:481-491.
23. Pierscionek B, Augusteyn RC. Protein distribution patterns in concentric layers from single bovine lenses: changes with development and ageing. *Curr Eye Res*. 1988;7:11-23.
24. Geary J. *Introduction to Lens Design: With Practical ZEMA Examples*. Richmond, VA. Willmann-Bell, Inc. 2002.
25. Rapuano C, Boxer Wachler BS, Davis EA, Donnenfeld ED. *Refractive Surgery*. San Francisco: American Academy of Ophthalmology; 2011.
26. Al-Ghoul KJ, Lane CW, Taylor VL, Fowler WC, Costello MJ. Distribution and type of morphological damage in human nuclear age-related cataracts. *Exp Eye Res*. 1996;62:237-251.
27. Costello MJ, Oliver TN, Cobo LM. Cellular architecture in age-related human nuclear cataracts. *Invest Ophthalmol Vis Sci*. 1992;33:3209-3227.
28. Michael R, Bron AJ. The ageing lens and cataract: a model of normal and pathological ageing. *Philos T R Soc B*. 2011;366:1278-1292.
29. Lou MF, Dickerson JE Jr. Protein-thiol mixed disulfides in human lens. *Exp Eye Res*. 1992;55:889-896.
30. Lou MF. Redox regulation in the lens. *Prog Retin Eye Res*. 2003;22:657-682.
31. Lou MF, Dickerson JE Jr, Tung WH, Wolfe JK, Chylack LT Jr. Correlation of nuclear color and opalescence with protein S-thiolation in human lenses. *Exp Eye Res*. 1999;68:547-552.
32. Sasaki H, Giblin FJ, Winkler BS, Chakrapani B, Leverenz V, Shu CC. A protective role for glutathione-dependent reduction of dehydroascorbic acid in lens epithelium. *Invest Ophthalmol Vis Sci*. 1995;36:1804-1817.
33. Pierscionek BK. The refractive index along the optic axis of the bovine lens. *Eye*. 1995;9:776-782.
34. Chaney WG, Spector A. HPLC analysis of lens GSH and GSSG. *Curr Eye Res*. 1984;3:345-350.
35. Giblin FJ, David LL, Wilmarth PA, Leverenz VR, Simpanya ME. Shotgun proteomic analysis of S-thiolation sites of guinea pig lens nuclear crystallins following oxidative stress in vivo. *Mol Vis*. 2013;19:267-280.
36. Padgaonkar VA, Lin LR, Leverenz VR, Rinke A, Reddy VN, Giblin FJ. Hyperbaric oxygen in vivo accelerates the loss of cytoskeletal proteins and MIP26 in guinea pig lens nucleus. *Exp Eye Res*. 1999;68:493-504.
37. Goldblum D, Brugger A, Haselhoff A, Schmickler S. Hyperopic shift in refraction in adults with aging. *Graefes Arch Clin Exp Ophthalmol*. 2013;251:2663.
38. Goldblum D, Brugger A, Haselhoff A, Schmickler S. Longitudinal change of refraction over at least 5 years in 15,000 patients. *Graefes Arch Clin Exp Ophthalmol*. 2013;251:1431-1436.
39. Pesudovs K, Elliott DB. Refractive error changes in cortical, nuclear, and posterior subcapsular cataracts. *Br J Ophthalmol*. 2003;87:964-967.
40. Samarawickrama C, Wang JJ, Burlutsky G, Tan AG, Mitchell P. Nuclear cataract and myopic shift in refraction. *Am J Ophthalmol*. 2007;144:457-459.
41. Bantsev V, Oriowo OM, Giblin FJ, Leverenz VR, Trevithick JR, Sivak JG. Effect of hyperbaric oxygen on guinea pig lens optical quality and on the refractive state of the eye. *Exp Eye Res*. 2004;78:925-931.
42. Wang H, Gao J, Sun X, et al. The effects of GPX-1 knockout on membrane transport and intracellular homeostasis in the lens. *J Membr Biol*. 2009;227:25-37.
43. Bettelheim FA, Lizak MJ, Zigler JS Jr. Synergetic response of aging normal human lens to pressure. *Invest Ophthalmol Vis Sci*. 2003;44:258-263.